

Inhibited oxidation in lowtemperature grown GaAs surface layers observed by photoelectron spectroscopy

T.B. Ng, D. B. Janes, D. McInturff, and J. M. Woodall

Citation: [Applied Physics Letters 69](#), 3551 (1996); doi: 10.1063/1.117242

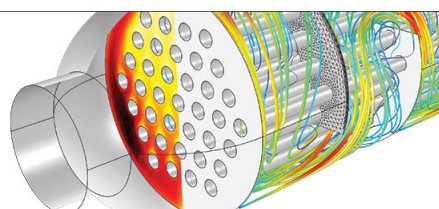
View online: <http://dx.doi.org/10.1063/1.117242>

View Table of Contents: <http://scitation.aip.org/content/aip/journal/apl/69/23?ver=pdfcov>

Published by the [AIP Publishing](#)

Over 700 papers & presentations on multiphysics simulation

[VIEW NOW ▶](#)



 COMSOL

Inhibited oxidation in low-temperature grown GaAs surface layers observed by photoelectron spectroscopy

T.-B. Ng, D. B. Janes,^{a)} D. McInturff, and J. M. Woodall

NSF MRSEC for Technology Enabling Heterostructure Materials and School of Electrical and Computer Engineering, Purdue University, West Lafayette, Indiana 47907

(Received 16 July 1996; accepted for publication 28 September 1996)

The surface oxidation characteristics of a GaAs layer structure consisting of a thin (10 nm) layer of low-temperature-grown GaAs (LTG:GaAs) on a heavily *n*-doped GaAs layer, both grown by molecular beam epitaxy, have been studied using x-ray photoelectron spectroscopy (XPS). Between the layer growth and XPS characterization, the unannealed LTG:GaAs sample and a control sample without the LTG:GaAs surface layer were exposed to the atmosphere. The rate of surface oxidation in the sample with a LTG:GaAs surface layer was significantly lower than the oxidation rate of the control sample. This direct observation of inhibited oxidation confirms the surface stability of comparable structures inferred from earlier electrical measurements. The inhibited surface oxidation rate is attributed to the bulk Fermi-level pinning and the low minority carrier lifetime in unannealed LTG:GaAs. © 1996 American Institute of Physics. [S0003-6951(96)03249-4]

Low-temperature grown GaAs (LTG:GaAs), i.e., layers grown by molecular beam epitaxy (MBE) at substrate temperatures of 250–300 °C, exhibit a number of interesting electronic properties associated with the excess arsenic incorporated during growth.¹ In as-grown LTG:GaAs material, the excess arsenic results in a large concentration (approximately $1 \times 10^{20} \text{ cm}^{-3}$) of point defects, primarily as arsenic antisites. The large concentration of point defects results in very short minority carrier lifetimes (<1 ps) and pinning of the bulk Fermi level near midgap.

In stoichiometric *n*-type GaAs, a significant layer of oxide (approximately 25 Å in thickness) forms rapidly upon exposure to atmosphere. In order to avoid this rapid oxidation, a number of passivation procedures have been employed, including As or S cap layers.^{2,3} Several recent experiments indicate that as-grown LTG:GaAs surface layers are more stable during air exposure than stoichiometric GaAs. *Ex situ* low resistance, nonalloyed contacts to *n*- and *p*-type GaAs have been demonstrated using a structure consisting of a thin layer of LTG:GaAs (2–5 nm) on a highly doped layer of normal growth temperature GaAs, both grown by MBE.⁴ Since LTG:GaAs layers as thin as 2 nm were effective in providing low-resistance Ohmic contacts following air exposure and an oxide etch, it can be inferred that the oxidation rate and oxide thickness in the LTG:GaAs layer are lower than those typically observed in stoichiometric GaAs following air exposure. The electronic properties of a comparable layer structure have been characterized following atmospheric exposure using scanning tunneling microscopy (STM).⁵ The observation of features associated with the GaAs band gap, along with the band of midgap states associated with the arsenic antisite defects, indicated that the LTG:GaAs layer did not significantly oxidize during approximately 1 h of air exposure or 25 h in dry nitrogen.⁵ While the contact resistance and STM studies provide evidence of inhibited surface oxidation, a more direct and quanti-

tative observation of the surface oxidation characteristics is essential for understanding the effect.

In order to provide a more direct observation of the oxidation characteristics of LTG:GaAs after air exposure, x-ray photoelectron spectroscopy (XPS) studies were performed on the layer structure shown in Fig. 1. This structure was grown in a Varian Gen II MBE on an epiready *n*⁺-GaAs (100) substrate, with a growth temperature of 580 °C for all layers except the not intentionally doped LTG:GaAs top layer, which was grown at 250 °C in order to incorporate excess arsenic. A silicon filament was used for the *n*-type doping, allowing doping concentrations of at least an order of magnitude higher than possible with conventional effusion cells. The growth rate for all layers was 1 μm/h. A control sample identical to the first sample, but without the LTG:GaAs surface layer, was prepared using the same growth conditions and was exposed to atmosphere simultaneously with the LTG:GaAs sample. XPS measurements were performed on the samples following exposure to atmosphere for (i) a period of approximately 60 min during transfer from the MBE system to the XPS chamber and (ii) an additional 31 h under illumination of fluorescent light in a clean air laminar flow chemical hood.

The XPS study was conducted in a Perkin–Elmer PHI 5400 ESCA system equipped with a monochromated source.

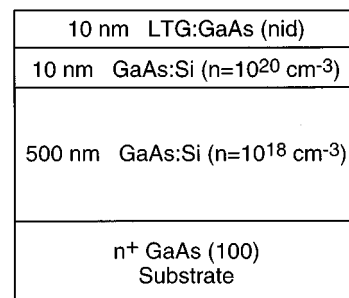


FIG. 1. A schematic diagram of the GaAs structure investigated. The control sample consisted of an identical structure, except the top layer was omitted.

^{a)}Electronic mail: janes@ecn.purdue.edu

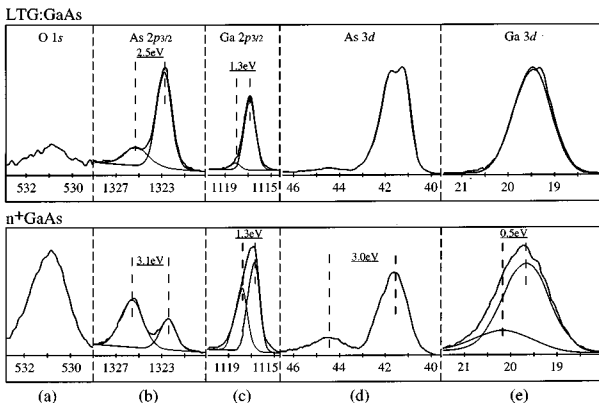


FIG. 2. X-ray photoelectron spectra for LTG:GaAs sample and control sample, following atmospheric exposure of approximately 60 min. (a) O 1 s peak, (b) As $2p_{3/2}$ peak, (c) Ga $2p_{3/2}$ peak, (d) As $3d$ peak, and (e) Ga $3d$ peak.

The XPS measurements were performed under ultrahigh vacuum (UHV), with a test chamber base pressure maintained in the mid- 10^{-10} Torr range. Samples are introduced into the chamber from a UHV transfer tube linking a series of other UHV instruments. The x-ray excitation used in this study is the Al $K\alpha$ line (1486.6 eV) generated by a dual anode x-ray source operating at 600 W and then passed through a silicon crystal monochromator. Electrons emitted from the samples are analyzed by an electron spectrometer at a 90° angle to the monochromator. The takeoff angle between the sample and the spectrometer analyzer input was kept fixed at 45° throughout. The electron binding energy in eV (horizontal axis of spectra) is calibrated using the Ag $3d_{5/2}$ peak at 367.9 eV.

Depth sensitivity of XPS depends on the takeoff angle and the binding energies of particular signal peaks. Higher binding energy corresponds to lower kinetic energy for the emitted electrons, which translates to shorter escape depth from the material and, hence, better surface sensitivity. For GaAs, the $2p_{3/2}$ and the $3d$ peaks, respectively, occupy the two ends of the binding energy range for the Al $K\alpha$ line excitation. The photoelectron escape depths for Ga and As $2p_{3/2}$ levels are given as 8 and 12 Å, respectively, as compared to about 25 Å for the Ga and As $3d$ levels.^{6,7} At a 45° takeoff angle, this corresponds to 2–3 ML for the $2p_{3/2}$ levels and 6 ML for the $3d$ levels. In order to be able to directly compare the XPS spectra of the LTG:GaAs sample with the n^+ -GaAs control sample, the escape depths in the LTG:GaAs, the n^+ -GaAs, and the oxides are assumed to be constant. This is reasonable since at the high energy of the photoelectrons, scattering by either impurities or traps are relatively insignificant.

Figure 2 presents the XPS spectra for the LTG:GaAs and the control samples after approximately 60 min of exposure to atmosphere. For regions where multiple peaks overlap, Gaussian peaks used to fit the data are shown along with the measured curves. Figure 2(a) shows the oxygen 1 s peak at 531 eV. The peak area for the LTG:GaAs is only about 20% of that for the control sample, indicating a significantly reduced level of surface oxidation in the LTG:GaAs sample. The effect is also evident in Figs. 2(b) and 2(c), which show

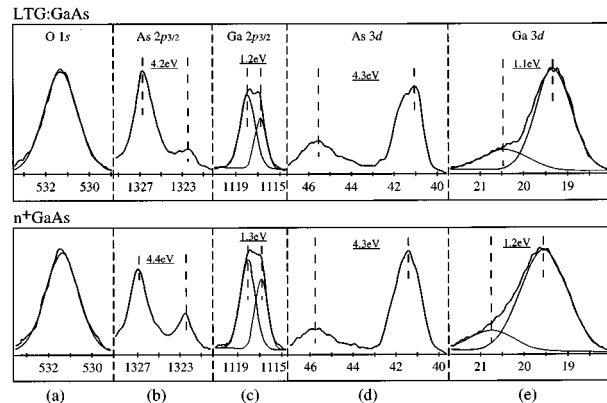


FIG. 3. X-ray photoelectron spectra for LTG:GaAs sample and control sample, following atmospheric exposure of approximately 31 h. (a) O 1 s peak, (b) As $2p_{3/2}$ peak, (c) Ga $2p_{3/2}$ peak, (d) As $3d$ peak, and (e) Ga $3d$ peak.

the As and Ga $2p_{3/2}$ level peaks. The As $2p_{3/2}$ peak of the control sample shows a well resolved Ga-bonded As peak at 1322.6 eV and an oxide peak at 3.1 eV towards higher binding energy, similar to cases reported for GaAs substrate surface after exposure to air^{8,9} and also after chemical preparations for MBE growth.¹⁰ This has been identified as As bonded to oxygen in a chemisorbed phase that relates to surface Fermi-level pinning.⁷ In contrast, the LTG:GaAs has a sharp Ga-bonded As peak and only a small shoulder at about 2.5 eV towards the higher energy side. In Fig. 2(c), the Ga $2p_{3/2}$ peak for LTG:GaAs can be curve fitted by a Gaussian peak at 1116.9 eV plus another small Gaussian peak at 1.3 eV higher binding energy, which consists of only about 8% of the total area under the curves. Using the same peak positions, curve fitting of the Ga $2p_{3/2}$ peak for the control sample shows the second peak to consist of about 40% of the total area. A comparison of the areas under the curves of corresponding peaks for the two samples indicates that the ratio between the area of the As peaks and that of the Ga peaks is larger for the LTG:GaAs sample: this behavior reflects the presence of significant excess As at the LTG:GaAs surface

Figures 2(d) and 2(e) show the more bulk sensitive As and Ga $3d$ level peaks that have been more widely studied in the literature. The As peak on the control sample again shows the characteristic oxide peak shifted by about 3.0 eV from the Ga-bonded As at 41.5 eV binding energy.^{6,10,11} This feature is hardly discernible on the LTG:GaAs. In Fig. 2(e), the Ga $3d$ peak for LTG:GaAs can be reasonably well approximated by a single Gaussian peak at 19.5 eV indicating relative absence of components other than the As-bonded Ga. In contrast, the corresponding peak for the control sample is wider and can be shown to consist of two Gaussian peaks 0.5 eV apart. The energy difference is smaller than the 1 eV commonly reported.^{6,10} Various explanations have been proposed for the observed broadening of the Ga $3d$ peak following surface oxidation of GaAs, not all of which involve formations of gallium oxides.¹²

Figure 3 illustrates the XPS spectra taken under the same conditions and parameters following the 31 h air exposure. The oxygen 1 s peaks for the LTG:GaAs and the control

sample, shown in Fig. 3(a) have become comparable in intensity and full width at half-maximum (FWHM) (1.8 eV), and can both be very well approximated by single Gaussian peaks. The observation strongly suggests that an equal amount of oxygen has been incorporated into the surface of both samples. This is also supported by the changes in the Ga $2p_{3/2}$, Ga $3d$, and As $3d$ peaks. By curve fitting, the Ga $2p_{3/2}$ peaks for both samples can be resolved into two Gaussian peaks about 1 eV apart with the shifted peak accounting for more than 60% of the total areas. Similarly for the Ga $3d$ peaks, the energy differences and the intensities of the shifted peaks are remarkably consistent even though the FWHM of the unshifted peak for LTG:GaAs is significantly narrower than the other sample. On the As $3d$ peaks, the oxidized As peaks have shifted to about 4.3 eV from the Ga-bonded As peak, which is approximately 1 eV higher than that for the control sample in Fig. 2(d). This implies that the As has evolved to a higher oxidized state, presumably As⁵⁺ as in As₂O₅. The same shift to higher energy is also observed on the As $2p_{3/2}$ peaks for both samples. However, in this case, the oxide peak on the LTG:GaAs has grown to a higher intensity than that of the control sample, accompanied by a corresponding reduction in the Ga-bonded As peak. Since the As $2p_{3/2}$ level is sensitive to only the first 2 ML, this would suggest that more of the oxide is concentrated on the surface of the LTG:GaAs sample, given that both samples incorporate a comparable amount of oxygen.

A qualitative picture of the oxidation mechanisms can explain the difference in oxidation characteristics between the LTG:GaAs sample and the control sample. The oxidation is primarily via photo-oxidation, in which six holes are required to oxidize a single GaAs pair.¹³ The rate of surface oxidation should, therefore, increase with increasing steady-state density of excess holes generated within a minority carrier (hole) diffusion length of the surface. In *n*-type stoichiometric GaAs, the minority carrier lifetime and diffusion length are relatively large, so the surface rapidly oxidizes during exposure to air under illumination. This process continues until the surface oxide thickness and midgap surface Fermi-level pinning are sufficient to stabilize the surface during air exposure.¹³ Kink sites, which are present on this surface, may also play a role in the decomposition of O₂ and H₂O at the surface.¹⁴ In unannealed LTG:GaAs, the bulk Fermi level is pinned approximately 0.4 eV below the conduction band edge,¹⁵ so the layer is light *n* type. However, the short minority carrier lifetime (100 fs) and corresponding short minority carrier diffusion length in the LTG:GaAs material result in a lower minority carrier concentration near the surface than would be found in stoichiometric material for the same illumination intensity and, therefore, a lower photo-oxidation rate. While midgap surface Fermi-level pinning may occur, the associated band bending will be small in both energy and spatial extent, due to the bulk Fermi-level pinning and the high space charge density associated with the antisite defects. There is also evidence that the (100) surface of LTG:GaAs does not reconstruct and, therefore, that kink sites do not form on this surface.¹⁶ Since the XPS technique is only sensitive to atoms located within a few monolayers of the surface, it is not possible to determine from this measurement whether the thickness of the oxide layer formed on the

LTG:GaAs sample after long air exposure is different from that of stoichiometric GaAs. However, scanning ellipsometry studies on comparable samples following air exposure indicate that the total oxide thickness on the LTG:GaAs surface is significantly less than that of an *n*-type surface.¹⁷

While the present study employed a 10 nm thick layer of LTG:GaAs on a heavily *n*-type GaAs layer, it is expected that the inhibited oxidation would be observed in nonalloyed LTG:GaAs layers as long as the thickness of the layer is sufficient to provide bulk behavior, i.e., a region in the LTG:GaAs in which flatband conditions exist. Based on the fact that layers of LTG:GaAs as thin as 2 nm are effective in providing low-resistance Ohmic contact layers to *n*-type GaAs,⁴ the minimum thickness of LTG:GaAs required to achieve this bulk behavior is believed to be less than 2 nm. Since thin layers of LTG:GaAs provide inhibited oxidation along with bulk Fermi-level pinning, this material should be suitable as a surface passivation layer for a variety of semiconductor materials.

In summary, XPS measurements have shown that LTG:GaAs surface layers oxidize less rapidly than layers of stoichiometric GaAs during air exposure. Layers of LTG:GaAs provide effective surface passivation due to the inhibited oxidation and bulk Fermi-level pinning in the material.

This work was partially supported by the NSF MRSEC program under Grant No. 9400415-DMR and the Army Research Office URI program under Contract No. DAAL03-G-0144. The authors would like to thank V. R. Kolagunta, Professor R. L. Gunshor, and Professor M. R. Melloch for technical assistance and helpful discussions.

- 1 M. R. Melloch, J. M. Woodall, E. S. Harmon, N. Otsuka, F. H. Pollak, D. D. Nolte, R. M. Feenstra, and M. A. Lutz, *Annu. Rev. Mater. Sci.* **25**, 547 (1995).
- 2 M. D. Pashley, K. W. Haberern, W. Friday, J. M. Woodall, and P. D. Kirchner, *Phys. Rev. Lett.* **60**, 2176 (1988).
- 3 S. Gwo, K.-J. Chao, A. R. Smith, C. K. Shih, K. Sadra, and B. G. Streetman, *J. Vac. Sci. Technol. B* **11**, 1509 (1993).
- 4 M. P. Patkar, T. P. Chin, J. M. Woodall, M. S. Lundstrom, and M. R. Melloch, *Appl. Phys. Lett.* **66**, 1412 (1995).
- 5 S. Hong, D. B. Janes, D. McInturff, R. Reifenberger, and J. M. Woodall, *Appl. Phys. Lett.* **68**, 2258 (1996).
- 6 E. Huber and H. L. Hartnagel, *Solid-State Electron.* **27**, 589 (1984).
- 7 W. E. Spicer, I. Lindau, P. Pianetta, P. W. Chye, and C. M. Garner, *Thin Solid Films* **56**, 1 (1979).
- 8 T. Ishikawa and H. Ikoma, *Jpn. J. Appl. Phys. 1* **31**, 3981 (1992).
- 9 H. Ohno, M. Motomatsu, W. Mizutani, and H. Tokumoto, *Jpn. J. Appl. Phys. 1* **34**, 1381 (1995).
- 10 J. Massies and J. P. Contour, *J. Appl. Phys.* **58**, 806 (1985); J. P. Contour, J. Massies, and A. Salettes, *Jpn. J. Appl. Phys. 1* **24**, L563 (1985).
- 11 W. Storm, D. Wolany, F. Schroder, G. Becker, B. Burkhardt, L. Wiedmann, and A. Benninghoven, *J. Vac. Sci. Technol. B* **12**, 147 (1994).
- 12 C. Y. Su, I. Lindau, P. Chye, P. R. Skeath, and W. E. Spicer, *Phys. Rev. B* **25**, 4045 (1982).
- 13 H. Gerischer, *J. Vac. Sci. Technol.* **15**, 1422 (1978).
- 14 W. A. Goddard III, J. J. Barton, A. Redondo, and T. C. McGill, *J. Vac. Sci. Technol.* **15**, 1274 (1978).
- 15 A. C. Warren, J. M. Woodall, P. D. Kirchner, X. Yin, X. Guo, F. H. Pollak, and M. R. Melloch, *J. Vac. Sci. Technol. B* **10**, 1904 (1992); H. Shen, F. C. Rong, R. Lux, J. Pamulapati, M. Taysing-Lara, M. Dutta, E. H. Poindexter, L. Calderon, and Y. Lu, *Appl. Phys. Lett.* **61**, 1585 (1992).
- 16 M. R. Melloch, D. C. Miller, and B. Das, *Appl. Phys. Lett.* **54**, 943 (1989).
- 17 F. Pollak (private communication).